

Thickness-dependent bulk properties and weak antilocalization effect in topological insulator Bi_2Se_3 Yong Seung Kim,^{1,2} Matthew Brahlek,¹ Namrata Bansal,³ Eliav Edrey,¹ Gary A. Kapilevich,¹ Keiko Iida,⁴ Makoto Tanimura,⁴ Yoichi Horibe,¹ Sang-Wook Cheong,¹ and Seongshik Oh^{1,*}¹*Department of Physics and Astronomy, The State University of New Jersey, Piscataway, New Jersey 08854, USA.*²*Department of Physics and Graphene Research Institute, Sejong University, Seoul 143-747, Korea*³*Department of Electrical and Computer Engineering, Rutgers, the State University of New Jersey, Piscataway, New Jersey 08854, USA*⁴*Research Department, Nissan Arc, Ltd., Yokosuka, Kanagawa 237-0061, Japan*

(Received 20 June 2011; published 26 August 2011)

We show that a number of transport properties in topological insulator (TI) Bi_2Se_3 exhibit striking thickness dependences over a range of up to five orders of thickness (3 nm–170 μm). Volume carrier density decreased with thickness, presumably due to diffusion-limited formation of selenium vacancies. Mobility increased linearly with thickness in the thin film regime and saturated in the thick limit. The weak antilocalization effect was dominated by a single two-dimensional channel over two decades of thickness. The sublinear thickness-dependence of the phase coherence length suggests the presence of strong coupling between the surface and bulk states.

DOI: [10.1103/PhysRevB.84.073109](https://doi.org/10.1103/PhysRevB.84.073109)

PACS number(s): 73.20.-r, 73.25.+i, 73.50.-h

Over the past few years, topological insulators (TI) have emerged as a new platform for coherent spin-polarized electronics. TIs are predicted to have an insulating bulk state and spin-momentum-locked metallic surface states.^{1–9} This spin-momentum-locking mechanism and their band structure topology are predicted to prevent the surface metallic states from being localized due to backscattering. Among the TIs discovered so far, Bi_2Se_3 is considered the most promising due to its near-ideal surface band structure,⁷ and its predicted surface states have been confirmed by a number of surface-sensitive probes.^{5,6,10–12} However, transport properties in this material have been far from the theoretical prediction of metallic surface states with insulating bulk states.^{12–14} Considering that the bulk and surface transport properties should exhibit very different thickness dependences, thickness-dependent transport studies can provide insights on both the bulk and surface states. Here we undertook extensive thickness-dependent studies of the transport properties in Bi_2Se_3 covering up to three orders of sample thickness, from which we made a number of critical findings that have been hidden in previous studies of Bi_2Se_3 .

For this study, we grew Bi_2Se_3 films with atomically sharp interfaces on undoped Si(111) substrates ($10 \times 10 \times 0.5 \text{ mm}^3$) by molecular beam epitaxy (MBE), covering more than three orders of thickness from 3 quintuple layers (QL, 1 QL $\approx 1 \text{ nm}$) through 3,600 QL. From a technological point of view, silicon is the most important substrate for electronic applications. However, interfaces between Bi_2Se_3 thin films and Si substrates have been plagued by disordered interfacial layers.^{14,15} In order to solve this problem, we developed a two-step growth scheme and obtained high-quality second-phase-free Bi_2Se_3 films on Si substrates with atomically sharp interfaces.¹⁶ Such an atomically sharp interface is crucial for reliable thickness-dependent studies for very thin samples. A cross-section transmission electron microscope (TEM) image of a Bi_2Se_3 film in Fig. 1(a) shows an atomically sharp interface between the film and the Si substrate. The sharp reflection high-energy electron diffraction (RHEED) pattern in the inset represents the high crystallinity of the Bi_2Se_3 film. Figure 1(b) shows x-ray diffraction (XRD) patterns for three different thicknesses. The peaks observed in the θ - 2θ scan are

consistent with the *c*-axis oriented Bi_2Se_3 phase. During the growth of the film, the gap between each line in the RHEED pattern, which is inversely proportional to the in-plane lattice constant of the film, changed to that of the bulk lattice constant during the first QL growth. This immediate lattice relaxation is attributed to the weak van der Waals-type bonding between the film and the substrate.

The transport measurements were carried out with the standard van der Pauw method with indium contacts on four square corners in a cryostat with magnetic field up to 9 T and a base temperature of 1.5 K; measurement errors due to the contact geometry are estimated to be less than 10%. For all films except for 3 QL, the R vs T curves in Fig. 2(a) showed metallic behavior at high temperature, but as the temperature dropped below 30 K, the resistance tended to increase slightly either due to strong electron-electron interaction in the two-dimensional (2D) limit¹⁷ or due to an impurity band in the bulk.¹⁸ The following measurements were all taken at a fixed temperature of 1.5 K with each sample exposed to air for less than 20 min to minimize air contamination; at this temperature, the undoped Si substrates were completely insulating and did not contribute to the transport measurements.

It is well known that the mobility of conventional thin films depends on the film thickness as $\mu(t) = \mu_\infty / (1 + 2(\lambda/t)(1-p))$, where μ_∞ is the mobility of the film when the thickness, *t*, is much larger than the mean free path, λ , with *p* representing the fraction of carriers reflecting specularly from the surface;¹⁹ this mobility drop originates from the reduction in the effective mean free path caused by diffuse scattering from the surfaces. Figure 2(b) shows that the mobility vs thickness data, obtained from Hall effect measurements, are in good agreement with this standard theory with $\mu_\infty \approx 3,000 \text{ cm}^2/\text{Vsec}$ and $\lambda(1-p) \approx 70 \text{ nm}$, except for the 3 QL data marked with a triangle. If the bulk of the film is insulating and the transport is entirely confined to the surfaces, the mobilities should be thickness independent except for very thin samples in which quantum tunneling between the top and bottom surfaces can degrade the surface states.^{20–22} The very observation of the conventional thickness dependence implies that the observed mobilities are dominated by the bulk instead of the surface transport.

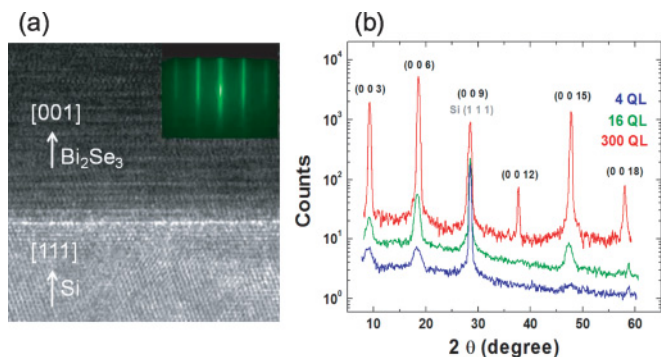


FIG. 1. (Color online) Epitaxial growth of Bi_2Se_3 film. (a) Cross-section TEM image of 32-QL film shows atomically sharp interface between Bi_2Se_3 and a Si substrate. Inset: RHEED pattern of the Bi_2Se_3 film. (b) High-resolution XRD pattern of three different films.

While the thickness dependence of the mobilities can be well understood by the standard surface scattering theory, the thickness dependence of the volume and sheet carrier densities plotted in Figs. 2(c)–2(d) is puzzling and unexpected. The volume carrier density (defined as the total sheet carrier density, obtained from the Hall measurement, divided by the sample thickness) decreases monotonically as the thickness

increases and scales as $t^{-0.5}$ over three orders of thickness range, from $5.3 \times 10^{19} \text{ cm}^{-3}$ for 3 QL to $1.6 \times 10^{18} \text{ cm}^{-3}$ for 3,600 QL. Little change occurred in these values even after the films were annealed in high selenium vapor pressures, up to six orders of magnitude higher than the normal growth conditions; this implies that the observed carrier densities are close to the absolute minimum values that are experimentally achievable in these pure Bi_2Se_3 films. We examined published data obtained from single crystal samples,¹⁸ and surprisingly these data points fell on the same curve, extending the trend up to five orders of thickness (3 nm–170 μm) with $2 \times 10^{17} \text{ cm}^{-3}$ for 170- μm -thick single crystal.¹⁸ Considering that two completely different sample formation processes, one through MBE growth and the other through peeling of bulk samples,¹⁸ result in the same thickness dependence suggests some fundamental mechanism behind this anomalous thickness dependence of the carrier densities. Another view of this anomaly is through the thickness dependence of the sheet carrier density. If we assume constant bulk volume carrier density (n_{BV}) and constant surface carrier density (n_{S}), the total sheet carrier density (n_{sheet}) should scale linearly with the sample thickness (t) such that $n_{\text{sheet}} = n_{\text{S}} + n_{\text{BV}}t$. In Fig. 2(d), the theoretical curve with $n_{\text{S}} = 2 \times 10^{13} \text{ cm}^{-2}$ and $n_{\text{BV}} = 1 \times 10^{18} \text{ cm}^{-3}$ was plotted for comparison with the experimental data. The observed data can in no way be

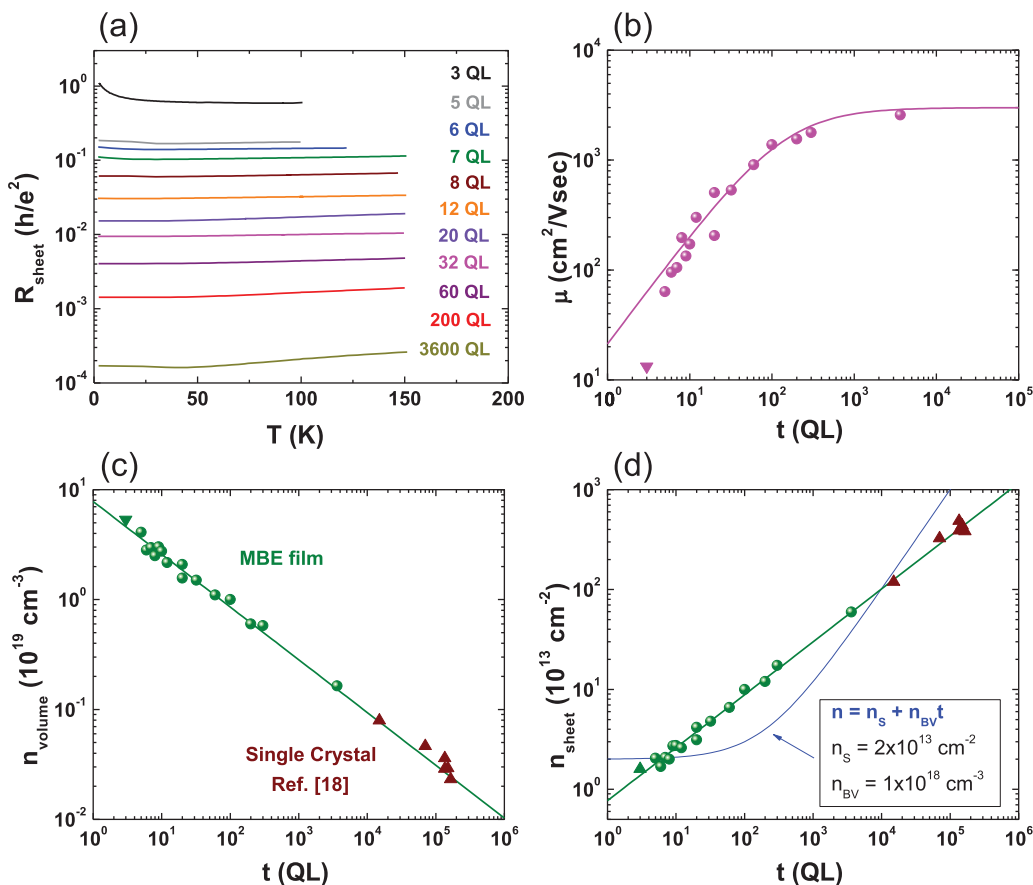


FIG. 2. (Color online) Thickness dependence of the transport properties of Bi_2Se_3 . (a) Resistance of Bi_2Se_3 films as a function of temperature with thickness ranging from 3 to 3,600 QL. Data above ~ 150 K are not shown here because they are affected by the parallel conduction of thermally excited carriers in the undoped silicon substrates. (b) Mobility. (c) and (d) Carrier density of electrons in Bi_2Se_3 films obtained by Hall measurement at 1.5 K. The solid curve in (b) is $\mu(t) = 3,000/(1 + 140/t)$, and the straight lines in (c) and (d) are illustrative guides.

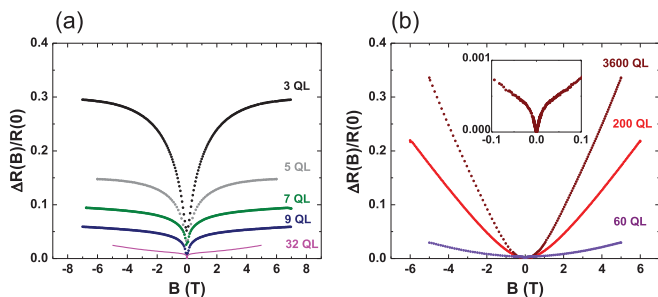


FIG. 3. (Color online) Normalized magnetoresistance. The magnetic field dependence of resistance at 1.5 K of (a) thin film from 3 to 32 QL and (b) thick film from 60 to 3,600 QL. Deep cusp in low-field regime is characteristic of the WAL effect. Parabolic field dependence is dominant in thick films. Inset of (b): zoomed-in view of the 3,600 QL data near zero field showing robustness of the WAL effect.

explained by this simple model, and instead the total sheet carrier density scales as $t^{0.5}$. This implies that the bulk volume carrier density is not constant but varies monotonically with its thickness over five orders of magnitude. Considering that either the TI surface state²⁰ or the surface band-bending effect²³ can never extend more than tens of nanometers, while the observed anomaly extends far beyond the micrometer scale, associating this observation with such an electronic mechanism seems unphysical. Because the volume carrier density mainly originates from the selenium vacancies,²⁴ this observation nominally implies that the volume density of selenium vacancies gradually increases as samples get thinner. The formation of selenium vacancies through diffusion seems to continuously occur even at room temperature, as confirmed by other group with x-ray photoelectron spectroscopy.²⁵ These observations suggest that formation of selenium vacancies in Bi_2Se_3 is thermodynamically favorable at room temperature, yet it occurs through a slow diffusion process, which is inevitably thickness dependent. This also implies that the measured carrier density of a sample depends on the time between sample fabrication and measurement, and so in order to maintain consistency, almost all samples reported here were measured on the day they were fabricated. In other words, the exact thickness dependence of the carrier densities, especially in the thin limit, may depend on when they are measured.

The magnetoresistance (MR) measurements provide another means to probe the TI properties. In Figs. 3(a)–3(b), the MR, defined as $(R(B)-R(0))/R(0)$, in the high-field regime is dominated by the parabolalike (B^2) dependence, originating from the Lorentzian deflection of carriers under perpendicular magnetic field²⁶ (recall that the electron executes cyclotron orbits, thereby shortening the mean free path, and thus increasing the resistance). The fact that this B^2 dependence is more pronounced in thicker samples suggests that it is a bulk-dominated effect.

In the low-field regime (<0.5 T) for thinner samples, the magnetoconductance (MC), as shown in Fig. 4(a), decreases sharply as the magnetic field is increased, which is typical of the weak antilocalization (WAL) effect.^{27,28} This WAL effect is the result of the strong spin-orbit coupling, which puts backscattering at the minimum when there is no magnetic field,

due to the time-reversal symmetry. As magnetic field increases, thus breaking the time-reversal symmetry, backscattering increases and leads to a sharp reduction in conductance. The low-field MC, $\Delta G(B) = G(B) - G(0)$, can be well fitted to the standard Hikami-Larkin-Nagaoka (HLN) theory for WAL:²⁹ $\Delta G(B) = A(e^2/h)[\ln(B_\phi/B) - \Psi(1/2 + B_\phi/B)]$, where A is a coefficient predicted to be $1/(2\pi)$ for each 2D channel, B_ϕ is the dephasing magnetic field, and $\Psi(x)$ is the digamma function. The dephasing magnetic field is related to the phase coherence length l_ϕ via¹⁷ $B_\phi = \hbar/(4el_\phi^2)$. Figures 4(b)–4(c) shows the fitting parameters as a function of thickness for 3–100 QL. Except for 3 QL, the fitting parameter A remains approximately constant around $1/(2\pi)$, while the parameter l_ϕ monotonically increases as samples get thicker. The parameter A being closer to $1/(2\pi)$ than $1/\pi$ nominally implies that the WAL effect over 5–100 QL is dominated by a single 2D channel.^{30,31} There are two possibilities for this observation. The first is that the WAL effect originates entirely from the reduced dimensionality of the metallic bulk state without any contribution from the surface states. The other is that the surface states contribute, but they couple strongly with the metallic bulk state and behave together as a single 2D system. We will show below that the thickness-dependence analysis of l_ϕ supports the latter. The WAL signal became too small to be of quantitative relevance as the thickness increased beyond 100 QL, but the spike in ΔG was still visible up to 3,600 QL as shown in the inset of Fig. 3(b), suggesting the robustness of the WAL effect.

Figure 4(c) shows that the phase coherence length l_ϕ scales as $t^{0.7}$. If the WAL effect originated entirely from the geometrically confined bulk state of the film without any surface state contribution, then l_ϕ should scale linearly with thickness in the thin film limit, just as the bulk-dominated mobility—a quantity proportional to a mean free path—presented in Fig. 2(b) scales almost linearly with the thickness over 5–100 QL. Therefore, the sublinear thickness dependence of l_ϕ suggests that there should be a considerable surface state contribution to the WAL signal and that the observed single channel effect must be due to strong coupling between the surface and bulk states. Now if the bulk of the film were insulating, then l_ϕ , being a surface property, had to be independent of the thickness—the surfaces should not change when the thickness changes. However, with conducting bulk states, the surfaces and bulk can interact with one another and lead to a thickness-dependent scattering mechanism. In other words, the thickness-dependent coherence length is a natural result of the metallic bulk states. According to this analysis, the thickness dependence of l_ϕ , denoted by α in $l_\phi \sim t^\alpha$, could be used as a figure of merit to tell how close certain TI materials are to an ideal TI; α should be zero for an ideal TI with the insulating bulk state, one for a topologically trivial strongly spin-orbit-coupled metal, and between zero and one for a nonideal TI with the metallic bulk state, approaching zero as the material gets closer to an ideal TI.

In summary, extensive thickness-dependent studies of the Bi_2Se_3 transport properties have led to a number of unexpected findings. The volume carrier density, which is commonly assumed to be thickness independent, decreased by more than two orders of magnitude over five orders of thickness, suggesting that selenium diffusion is highly thickness de-

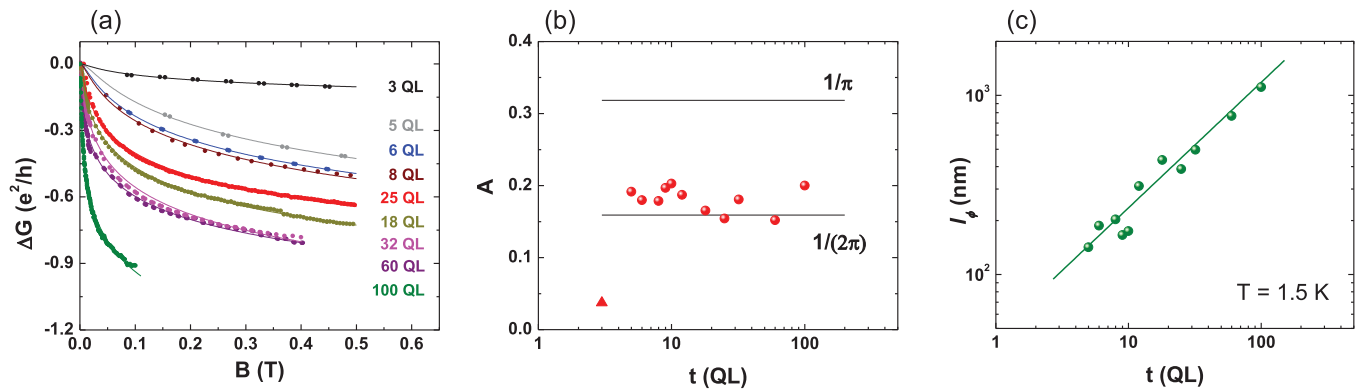


FIG. 4. (Color online) Weak antilocalization effect. (a) The HLN fitting of the change in conductance in low-field regime from 3 to 100 QL. (b) Above 5 QL, the coefficient A is almost thickness independent, close to a single channel WAL contribution, that is $1/(2\pi)$. (c) The phase coherence length increases as $t^{0.7}$ with the sample thickness.

pendent and active even at room temperature. The mobility increased linearly with thickness in the thin film regime and saturated as the samples got thicker, suggesting that the surface scattering effect limits the mean free path in the thin limit. The WAL effect was dominated by a single 2D channel over two decades of thickness. The sublinear thickness dependence of the phase coherence length supports the presence of the surface states and provides a figure of merit, characterizing the level of interaction between the surface and bulk states.

Our observations suggest that interactions between the bulk and surface states have profound effects on their transport properties.

We thank Keun Hyuk Ahn for reviewing the manuscript before submission. This work is supported by IAMDN of Rutgers University, National Science Foundation (NSF DMR-0845464) and Office of Naval Research (ONR N000140910749).

*Corresponding author: ohsean@physics.rutgers.edu

¹M. Z. Hasan and C. L. Kane, *Rev. Mod. Phys.* **82**, 3045 (2010).

²X. L. Qi and S. C. Zhang, *Phys. Today* **63**, 33 (2010).

³J. E. Moore, *Nature* **464**, 194 (2010).

⁴D. Hsieh, Y. Xia, D. Qian, L. Wray, J. H. Dil, F. Meier, J. Osterwalder, L. Patthey, J. G. Checkelsky, N. P. Ong, A. V. Fedorov, H. Lin, A. Bansil, D. Grauer, Y. S. Hor, R. J. Cava, and M. Z. Hasan, *Nature* **460**, 1101 (2009).

⁵H. L. Peng, K. J. Lai, D. S. Kong, S. Meister, Y. L. Chen, X. L. Qi, S. C. Zhang, Z. X. Shen, and Y. Cui, *Nat. Mater.* **9**, 225 (2010).

⁶Y. Xia, D. Qian, D. Hsieh, L. Wray, A. Pal, H. Lin, A. Bansil, D. Grauer, Y. S. Hor, R. J. Cava, and M. Z. Hasan, *Nat. Phys.* **5**, 398 (2009).

⁷H. J. Zhang, C. X. Liu, X. L. Qi, X. Dai, Z. Fang, and S. C. Zhang, *Nat. Phys.* **5**, 438 (2009).

⁸Y. L. Chen, J. G. Analytis, J. H. Chu, Z. K. Liu, S. K. Mo, X. L. Qi, H. J. Zhang, D. H. Lu, X. Dai, Z. Fang, S. C. Zhang, I. R. Fisher, Z. Hussain, and Z. X. Shen, *Science* **325**, 178 (2009).

⁹D. Hsieh, D. Qian, L. Wray, Y. Xia, Y. S. Hor, R. J. Cava, and M. Z. Hasan, *Nature* **452**, 970 (2008).

¹⁰T. Hanaguri, K. Igarashi, M. Kawamura, H. Takagi, and T. Sasagawa, *Phys. Rev. B* **82**, 081305 (2010).

¹¹P. Cheng, C. L. Song, T. Zhang, Y. Y. Zhang, Y. L. Wang, J. F. Jia, J. Wang, Y. Y. Wang, B. F. Zhu, X. Chen, X. C. Ma, K. He, L. L. Wang, X. Dai, Z. Fang, X. C. Xie, X. L. Qi, C. X. Liu, S. C. Zhang, and Q. K. Xue, *Phys. Rev. Lett.* **105**, 076801 (2010).

¹²J. G. Analytis, R. D. McDonald, S. C. Riggs, J.-H. Chu, G. S. Boebinger, and I. R. Fisher, *Nat. Phys.* **6**, 960 (2010).

¹³N. P. Butch, K. Kirshenbaum, P. Syers, A. B. Sushkov, G. S. Jenkins, H. D. Drew, and J. Paglione, *Phys. Rev. B* **81**, 241301 (2010).

¹⁴H. D. Li, Z. Y. Wang, X. Kan, X. Guo, H. T. He, Z. Wang, J. N. Wang, T. L. Wong, N. Wang, and M. H. Xie, *New J. Phys.* **12**, 103038 (2010).

¹⁵G. H. Zhang, H. J. Qin, J. Teng, J. D. Guo, Q. L. Guo, X. Dai, Z. Fang, and K. H. Wu, *App. Phys. Lett.* **95**, 053114 (2009).

¹⁶N. Bansal, Y. S. Kim, E. Edrey, M. Brahlek, Y. Horibe, K. Iida, M. Tanimura, G.-H. Li, T. Feng, H.-D. Lee, T. Gustafsson, E. Andrei, and S. Oh, e-print [arXiv:1104.3438](https://arxiv.org/abs/1104.3438) (2011).

¹⁷M. Liu, C.-Z. Chang, Z. Zhang, Y. Zhang, W. Ruan, K. He, L.-l. Wang, X. Chen, J.-F. Jia, S.-C. Zhang, Q.-K. Xue, X. Ma, and Y. Wang, *Phys. Rev. B* **83**, 165440 (2011).

¹⁸J. G. Analytis, J. H. Chu, Y. L. Chen, F. Corredor, R. D. McDonald, Z. X. Shen, and I. R. Fisher, *Phys. Rev. B* **81**, 205407 (2010).

¹⁹A. Elshabini and F. D. Barlow, *Thin Film Technology Handbook* (McGraw-Hill, New York, 1998) p. 4–9.

²⁰J. Linder, T. Yokoyama, and A. Sudbø, *Phys. Rev. B* **80**, 205401 (2009).

²¹Y. Zhang, K. He, C. Z. Chang, C. L. Song, L. L. Wang, X. Chen, J. F. Jia, Z. Fang, X. Dai, W. Y. Shan, S. Q. Shen, Q. A. Niu, X. L. Qi, S. C. Zhang, X. C. Ma, and Q. K. Xue, *Nat. Phys.* **6**, 584 (2010).

²²H.-Z. Lu, W.-Y. Shan, W. Yao, Q. Niu and S.-Q. Shen, *Phys. Rev. B* **81**, 115407 (2010).

²³M. Bianchi, D. Guan, S. Bao, J. Mi, B. B. Iversen, P. D. C. King, and P. Hofmann, *Nat. Commun.* **1**, 128 (2010).

²⁴Y. S. Hor, A. Richardella, P. Roushan, Y. Xia, J. G. Checkelsky, A. Yazdani, M. Z. Hasan, N. P. Ong, and R. J. Cava, *Phys. Rev. B* **79**, 195208 (2009).

²⁵D. Kong, K. Lai, H. Peng, J. G. Analytis, S. Meister, Y. Chen, H.-J. Zhang, I. R. Fisher, Z.-X. Shen, and Y. Cui, *ACS Nano* **5**, 4698 (2011).

- ²⁶J. M. Ziman, *Electrons and Phonons: The Theory of Transport Phenomena in Solids* (Clarendon Press, Oxford, 1960) p. 504.
- ²⁷J. Chen, H. J. Qin, F. Yang, J. Liu, T. Guan, F. M. Qu, G. H. Zhang, J. R. Shi, X. C. Xie, C. L. Yang, K. H. Wu, Y. Q. Li, and L. Lu, *Phys. Rev. Lett.* **105**, 176602 (2010).
- ²⁸J. G. Checkelsky, Y. S. Hor, R. J. Cava, and N. P. Ong, *Phys. Rev. Lett.* **106**, 196801 (2011).
- ²⁹S. Hikami, A. Larkin, and Y. Nagaoka, *Prog. Theor. Phys.* **63**, 707 (1980).
- ³⁰J. Chen, X. Y. He, K. H. Wu, Z. Q. Ji, L. Lu, J. R. Shi, J. H. Smet, and Y. Q. Li, *Phys. Rev. B* **83**, 241304 (2011).
- ³¹H. Steinberg, J.-B. Laloë, V. Fatemi, J. S. Moodera, and P. Jarillo-Herrero, e-print [arXiv:1104.1404](https://arxiv.org/abs/1104.1404) (2011).